



Ciprofloxacin adsorption onto *Azolla filiculoides* activated carbon from aqueous solutions

Davoud Balarak^a, Marzieh Baniasadi^b, Seung-Mok Lee^{c,*}, Moo Joon Shim^{c,*}

^aDepartment of Environmental Health, Health Promotion Research Center, Zahedan University of Medical Sciences, Zahedan, Iran, Tel. +98-54-3329-5765; email: dbalarak2@gmail.com

^bStudent Research Committee, Zahedan University of Medical Sciences, Zahedan, Iran

^cDepartment of Environmental Engineering, Catholic Kwandong University, Gangneung, Korea, Tel. +82-33-649-7535/ +82-33-649-7110; emails: moojoonshim@gmail.com (M.J. Shim), leesm@cku.ac.kr (S.-M. Lee)

Received 30 July 2020; Accepted 27 December 2020

ABSTRACT

The adsorption of ciprofloxacin (CIP) from aqueous solutions by *Azolla filiculoides* activated carbon (AFAC) was studied in a batch adsorption system. Results revealed that at CIP concentration of 10 mg/L, AFAC dose of 2.5 g/L, the contact time of 75 min, the temperature of 50°C, the CIP removal reached about 99.1%. Langmuir, Freundlich and Dubinin–Radushkevich isotherm models were studied to determine the adsorption mechanism. Langmuir isotherm best fits the equilibrium adsorption data and the maximum capacity was 35.14 mg/g. The adsorption intensity obtained from the Freundlich model and the energy of adsorption obtained from the Dubinin–Radushkevich model (2.25 kJ/mol) suggested that physisorption dominates the adsorption of CIP onto the AFAC. All the error functions in the Langmuir isotherms showed that the error in the least. Thermodynamic parameters were calculated for the CIP–AFAC system and the positive value of ΔH° (52.7 kJ/mol) and negative values of ΔG° (–0.079 to –5.61) showed that the adsorption was endothermic, spontaneous and physical in nature. The results of sequential adsorption–desorption showed that the AFAC could be successfully reused for five cycles. The characteristic results showed that AFAC can be employed as an alternative to commercial adsorbents in the removal of antibiotics from wastewater.

Keywords: Adsorption; *Azolla filiculoides* activated carbon; Ciprofloxacin; Error analysis

1. Introduction

Pharmaceutical residues, which are emerging contaminants, exist in various water columns and have gained the attention of researchers due to their toxicity to aquatic organisms [1,2]. These compounds are medicines used in humans and animals and introduced into water systems because wastewater treatments may not completely remove them [3,4]. The presence of antibiotic residues in the sewage treatment plants poses a problem due to the reasons such as increased risks to human health from the development of antibiotic-resistant microorganisms if antibiotics

are present in sublethal concentrations of the pathogens in sewage.

Ciprofloxacin (CIP), fluoroquinolone antibiotic, has been used to treat both human and animal diseases [5]. CIP is widely used around the world with a cumulative sales income of more than \$1 billion [6,7]. A large amount of CIP is excreted from human and animal bodies' incomplete metabolism [8,9]. The CIP concentrations in effluents of wastewater treatment plants range from ng to mg/L [10]. In Iran, the amount of CIP antibiotics in hospital wastewater in the range of 20 µg/L to 20 mg/L has been detected in sewage effluents [10]. The secondary treatment of

* Corresponding authors.

wastewater is often based on bacterial activity such as the activated sludge process; the existing facilities are often not designed completely to remove antibiotic residues from the sewage through the treatment process [11].

Several methods (e.g., chemical precipitation, chemical oxidation or reduction, electrochemical treatment, ion exchange, reverse osmosis, filtration, and electrocoagulation) have been employed to treat wastewaters containing antibiotics [11,12]. However, some studies reported that these methods have several problems such as high energy requirements, inefficient antibiotics removal, generation of toxic sludge, and expensive equipment [13,14]. Therefore, new efficient and cost-effective technologies to eliminate antibiotics should be developed [15,16].

Adsorption is known as the simplest and economical method to remove dyes from wastewaters [17–19]. Activated carbon produced from agricultural waste (e.g., orange peel, jute fiber, wheat shells, soy meal hull, rice husk, canola husk, activated date pit, *Lemna minor*, and bamboo dust) has been widely used as an adsorbent [20–25]. Activated carbons, with their high surface area and capacity, microporous structure and chemical nature of their surface, are potential adsorbents for the removal of different antibiotics from industrial wastewaters [26]. However, the main disadvantages of activated carbon are high production and regeneration costs. Interestingly, it has been found that adsorption of antibiotics onto activated carbon is significantly influenced by characteristics of the activated carbon [27]. Therefore, the method of carbon activation aimed at improving its adsorption capability and thus reducing the rate of activated carbon consumption to reduce the cost of activated carbon adsorption making more it cost-effective.

Azolla filiculoides is one the famous aquatic algae and found in rice paddy fields and which has been used in various studies to remove a different kinds of pollutants [28]. The *Azolla filiculoides* have been shown a suitable potential to grow in wastewater and absorb inorganic and organic material from the effluents. The rapid growth of *Azolla filiculoides* is the main property that is assumed as an issue produced by this alga [29,30]. The use of this alga as an inexpensive and effortlessly available adsorbent can play a significant role in the alleviation of the severity of this problem.

Therefore, the objective of this study is to investigate the availability of *Azolla filiculoides* activated carbon (AFAC) as an adsorbent for the removal of CIP from aqueous solutions. For this study, the influence of several factors (e.g., contact time, AFAC amount, temperature CIP concentration, and shaking speed) on the removal efficiency of CIP was investigated. The kinetic, isotherm and thermodynamic models were applied to explain the adsorption behavior. Also, error functions were also calculated.

2. Material and methods

2.1. Reagents

Ciprofloxacin ($C_{17}H_{18}FN_3O_3 \cdot HCl$, molecular weight 331.3 g/mol, purity >98%) was supplied from Sigma-Aldrich (USA), with the molecular structure of CIP given in Fig. 1. The removal experiments were carried out using an aqueous solution of CIP to minimize interference by other elements

that exist in the wastewater. The stock solution (1,000 mg/L) was produced by dissolving CIP in distilled water. Different concentrations of CIP (10–100 mg/L) were obtained by diluting the stock solution with distilled water. In addition, the pH of the solution was adjusted using 0.1 N of HCl and NaOH solution to achieve a neutral pH (pH = 6.5).

2.2. Preparation and characterization of the AFAC adsorbent

Marine alga, *Azolla filiculoides*, used for the preparation of the activated carbon, was collected from the Anzali Wetland, Iran. This *Azolla filiculoides* was washed with distilled water and dried at room temperature for a week. The dried *Azolla filiculoides* was then milled and separated by manually shaking stainless steel mesh screens with the opening of standard 0.45 mm. Thus, for the production of activated carbon, 5 g of the dried *Azolla filiculoides* were weighed with a digital scale and stirred in 40 mL of $ZnCl_2$ solution for 6 h and dried in an electric oven at 105°C for 24 h. Then, the mixture was put in a vertical stainless-steel reactor under high-purity nitrogen with a flow rate of 300 cm^3/min , heated to a final temperature of 450°C, and finally left to be activated for 1 h.

The residual $ZnCl_2$ was removed with 0.05 M HCl solution after the mixture was completely dried in an oven at 105°C. Subsequently, the final AFAC was dried in an oven at 105°C for 24 h after it was rinsed with the distilled water. The yield of the prepared AFAC was calculated based on the following equation [26,27]:

$$Y(\%) = \frac{W_{AC}}{W} \times 100 \quad (1)$$

where W_{AC} and W are the weights of carbon products and dried pods.

2.3. Batch adsorption experiments

The adsorption tests were conducted using 250 mL Erlenmeyer flasks containing 100 mL of CIP ion solution of different concentrations (10–100 mg/L). The desired amount of AFAC was added to the solution and the flasks were agitated on an electrically thermostatic shaker at a speed of 120 rpm. The effect of different experimental parameters such as AFAC dose (0.25–4 g/L), initial concentration of CIP (10–100 mg/L), shaking speed (25–200 rpm), contact time (10–150 min) and temperature (20°C–50°C) at fixed pH 6.5

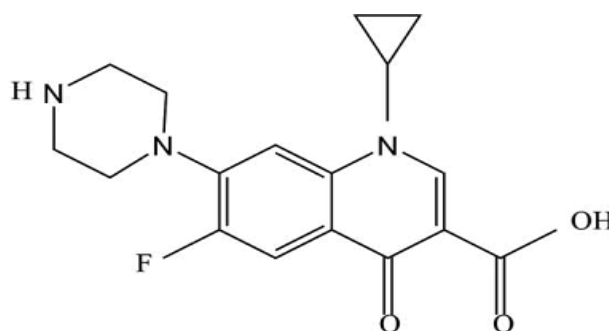


Fig. 1. Structure of ciprofloxacin.

was evaluated for sorption of CIP by AFAC. At the end of the experiment, the contents of the flasks were filtered using a Whatman filter paper. All the experimental works were conducted in triplicates for all the conditions in this study.

CIP concentration of all samples was determined by high-performance liquid chromatography (HPLC) (C_{18} ODS column) with a UV detector 2006 at a wavelength of 277 nm. The mobile phase was 0.05 M phosphoric acid/acetonitrile with a volumetric ratio of 87/13 and an injection flow rate of 1 mL/min.

The CIP uptake capacity q_e was calculated using general Eq. (2) [28,29]:

$$q_e = \frac{(C_0 - C_e) \times V}{M} \quad (2)$$

where q_e is the CIP uptake (mg/g AFAC), V the volume of CIP containing solution in contact with the AFAC (L), C_0 and C_e are the initial and equilibrium (residual) concentrations of CIP in the solution respectively (mg/L), and M is the amount of added AFAC (g).

2.4. Desorption and regeneration studies

The regeneration and reusability of AFAC composites were investigated by adsorption–desorption experiments that were conducted in a batch process. An amount of 2.5 g/L AFAC was added to 10 mL of CIP solution (10 mg/L). Then, desorption of CIP-loaded AFAC was accomplished with

100 mL of HCl, H_2SO_4 , H_2O solutions and vibrating for 90 min, and the solutions were filtered and concentrations of CIP in the aqueous solution were determined by HPLC method.

Thereafter, to regenerate the adsorption sites of adsorbent, AFAC composites after desorption were recovered by adding the adsorbent to 100 mL of a 0.5 M H_2SO_4 solution and vibrating for 1.5 h, and the adsorbent was then separated and dried. The adsorbent regenerated using H_2SO_4 was reused in the next adsorption cycle under the same adsorption conditions, and five adsorption regeneration cycles were carried out to evaluate the adsorbent reusability. In particular, the results of experiments were also used to compare with those of adsorbents without desorption and regeneration. Desorption (%) was calculated according to Eq. (3):

$$\text{Desorption (\%)} = \frac{\text{desorption ion}}{\text{adsorption ion}} \times 100 \quad (3)$$

3. Results and discussion

The characteristics of AFAC are summarized in Table 1. The prepared AFAC had a specific surface area of 716.4 m^2/g , total pore volume of 0.481 cm^3/g , a porosity of 51.2%, and a bulk density of 0.693 g/cm^3 . The scanning electron microscopy (SEM) of AFAC before and after adsorption are indicated in Fig. 2. The pores of the adsorbent after adsorption were filled with CIP molecules (Fig. 2). In addition, the SEM image showed that characteristics of the

Table 1
Characteristics of the AFAC

Specific surface area	Average pore diameter	Porosity	Pore volume	Moisture	Bulk density
716.4 m^2/g	41.3 nm	51.2%	0.481 cm^3/g	2.21%	0.693 g/cm^3
C%	H%	N%	O%	Y	%Ash
51.2%	4.18%	0.725	40.71	44.7%	2.84

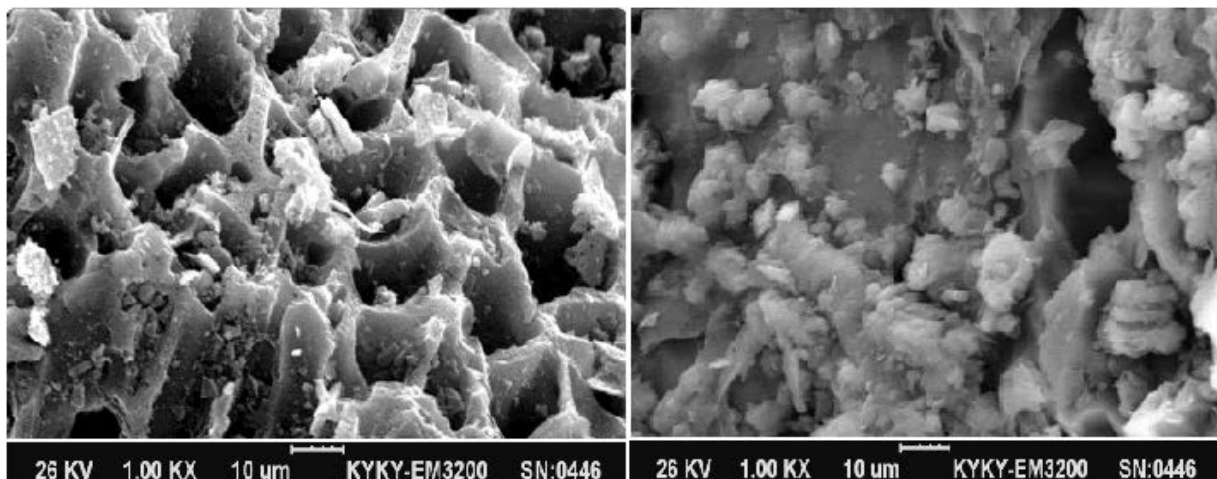


Fig. 2. SEM images of (a) AFAC before and (b) after CIP adsorption.

starting materials largely influenced carbon texture and porosity development.

Fig. 3 illustrated the N_2 adsorption and pore size distribution of AFAC. A type IV isotherm was revealed by the hysteresis loop at high P/P_0 values. The pore diameter range of AFAC was 4–5 nm. Fourier-transform infrared spectroscopy spectrum of AFAC is given in Fig. 4. The absorption peaks are at $1,140\text{ cm}^{-1}$ associated with C–O stretching vibration, $1,450\text{--}1,600\text{ cm}^{-1}$ associated with C=C stretching vibration (alkyne groups), $2,320\text{ cm}^{-1}$ associated with O=C=O stretching vibration, $1,720$ and $1,740\text{ cm}^{-1}$ associated with existence of carboxylic groups, and $2,830$ and $2,870\text{ cm}^{-1}$ related with C–H (stretching vibrations of CH_3 and CH_2 functional groups).

3.1. Effect of contact time

The percentage removal of CIP is a function of contact time. The percentage of CIP removal increased with increasing contact time (Fig. 5). The uptake of CIP was rapid for the first 30 min and after 60 min, the amount of CIP adsorbed

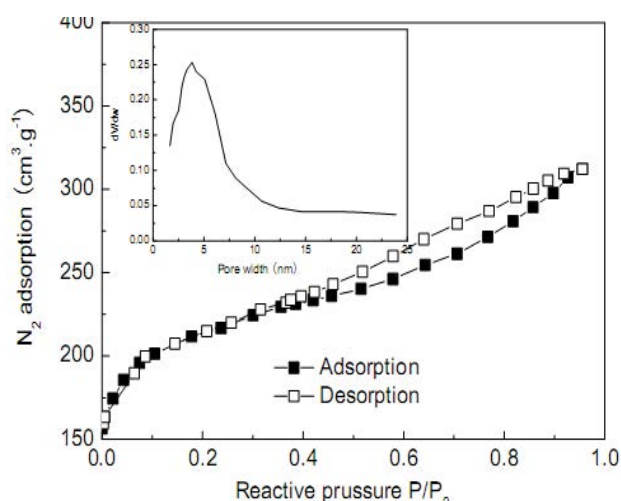


Fig. 3. N_2 adsorption–desorption isotherms. Inset: the Barrett–Joyner–Halenda pore size distribution curves.

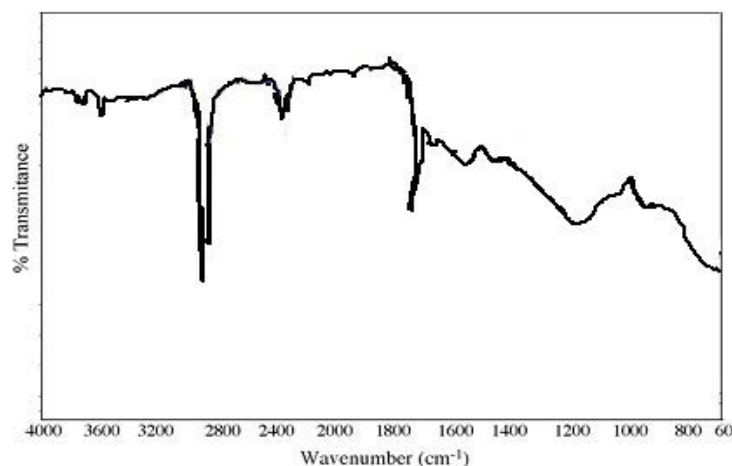


Fig. 4. Fourier-transform infrared spectra of produced AFAC.

remained almost constant. Hence, in the present study, 60 min was chosen as the equilibrium time. At the beginning of the reaction, adsorption was fast because many vacant sites were available [30,31]. In contrast, the slow adsorption was possibly due to insufficient vacant sites [32,33]. Percentage adsorption increased from 37.1 to 94.25 during a contact time period from 10 to 60 min.

3.2. Effect of shaking speed

As the shaking speed increased from 25 to 200 rpm, the adsorption capacity also increased from 12.04 to 35.56 mg/g for CIP (Fig. 6). The adsorption rate increased as the shaking speed increased possibly because the boundary thickness around the adsorbent decreased. Therefore, with increasing shaking speed, the concentration on CIP ions near the adsorbent surface would also increase [34,35].

3.3. Effect of adsorbent dose

The effect of adsorbent dosage on CIP removal from the antibiotics solution of 50 mg/L was evaluated by varying the adsorbent dosage (0.25–4 g/L). The adsorption increased with increasing AFAC dosage (Fig. 7). The percentage removal increased from 48.5% to 81.95% when AFAC dose increased from 0.25 to 2.5 g/L. Therefore, the optimum AFAC dosage was taken as 2.5 g/L for further experiments. The increase in percentage removal could be attributed to the fact that as AFAC dosage increases, more adsorption sites are available for CIP, thus enhancing the uptake [36,37]. However, on further increasing the AFAC dose, the ratio of adsorbent capacity to the unit weight of AFAC reduced, thus causing a decrease in CIP uptake (q_e) value. This could be because there are interactions of several factors (e.g., availability of solute, electrostatic interactions and interference between binding sites) [38,39].

3.4. Adsorption kinetics

Pseudo-first-order, pseudo-second-order and intra-particle-diffusion kinetic models were applied to study the adsorption rate and mechanism. The linear form of

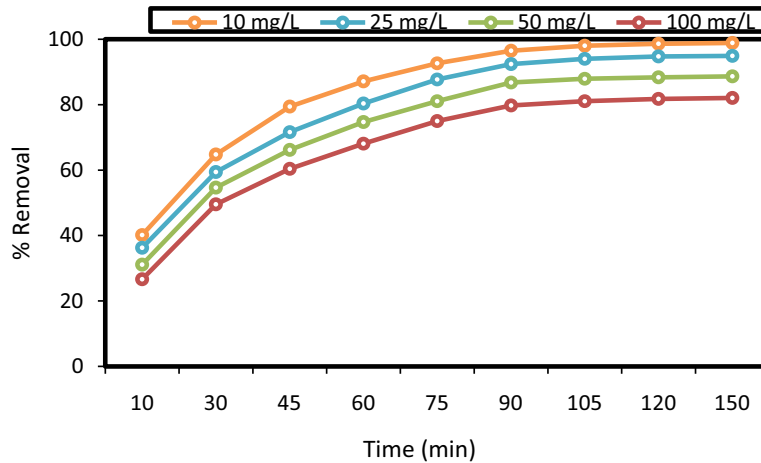


Fig. 5. Effect of contact time on CIP removal (pH = 6.5; AFAC dosage 2.5 g/L; temperature = 28°C ± 2°C).

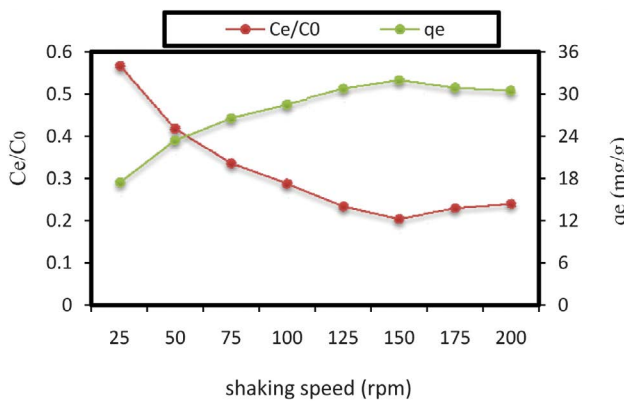


Fig. 6. Effect of shaking speed on CIP adsorption ($C_0 = 100$ mg/L; time = 90 min; pH = 6.5; temperature = 28°C ± 2°C; AFAC dosage 2.5 g/L).

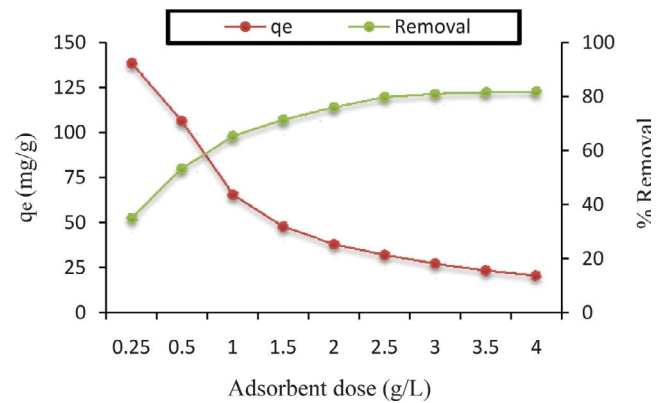


Fig. 7. Effect of adsorbent dosage on CIP adsorption ($C_0 = 100$ mg/L; time = 90 min; pH = 6.5; temperature = 28°C ± 2°C).

the pseudo-first-order kinetic is generally expressed as Eq. (4) [40,41]:

$$\log(q_e - q_t) = \log q_e - \frac{K_1}{2.303} t \quad (4)$$

where q_e and q_t are the amount of CIP adsorbed at equilibrium and time t , respectively, and K_1 represents the rate constant of adsorption. The respective values are given in Table 2.

Experimental and calculated q_e values were different even though R^2 values seemed linear (figure not shown), suggesting that biosorption of AFAC does not follow a pseudo-first-order kinetic model. The kinetics of adsorption is also described by pseudo-second-order kinetic equation expressed as Eq. (5) [42]:

$$\frac{t}{q_t} = \frac{1}{K_2 q_e^2} + \frac{t}{q_e} \quad (5)$$

where K_2 is the second-order rate constant of adsorption. The plot (Fig. 8) of t/q_t vs. t of the above equation showed a linear relationship between t/q_t and t . The rate constants and the correlation coefficients were calculated and

summarized in Table 2. The value of the correlation coefficient R^2 for the pseudo-second-order adsorption model was relatively high (>0.997) at all concentrations. Also, q_e (calculated) using pseudo-second-order model is equal to that obtained experimentally. These values indicated that biosorption follows the pseudo-second-order mechanism and that chemisorption controls the rate of biosorption.

The Weber and Morris intraparticle diffusion model was used to define the diffusion mechanism. This is given as Eq. (6) [43]:

$$q_t = Kt^{0.5} + I \quad (6)$$

where I is the intercept and K is the intraparticle diffusion rate constant. As the intercept increases, the contribution of the surface sorption increases in the rate-controlling step.

The plots not passing through the origin shows that intraparticle diffusion took place in the adsorption process, but it was not the only parameter controlling the adsorption process. However, as seen in Fig. 9, the second adsorption phase is characterized by intraparticle diffusion. The intercept I are related to the boundary layer thickness. The highest boundary layer thickness was observed from

Table 2
Kinetic models and error analysis parameters for CIP adsorption onto AFAC

Kinetic models	Parameters	CIP concentration (mg/L)			
		10	25	50	100
Pseudo-first-order	$q_{e,cal}$ (mg/g)	1.25	4.17	11.81	20.65
	$q_{e,exp}$ (mg/g)	3.95	9.63	18.27	34.53
	K_1	0.398	0.312	0.241	0.169
	R^2	0.812	0.829	0.794	0.841
	SSE	14.15	11.81	18.44	14.91
	SAE	11.21	18.19	20.17	14.85
	ARE %	14.85	19.24	17.41	22.18
	HYBRID	6.95	8.71	9.82	7.44
	MPSD	12.45	15.32	14.49	13.89
Pseudo-second-order	$q_{e,cal}$ (mg/g)	3.64	8.98	18.05	33.17
	$q_{e,exp}$ (mg/g)	3.95	9.63	18.27	34.53
	K_2	0.0086	0.0073	0.0064	0.0052
	R^2	0.998	0.997	0.998	0.999
	SSE	7.463	6.591	4.712	4.251
	SAE	6.925	7.526	5.532	2.749
	ARE	2.145	3.411	2.846	1.734
	HYBRID	9.341	6.598	4.343	5.812
	MPSD	8.729	7.457	9.325	3.672
	K	0.918	0.784	0.625	0.541
Intraparticle diffusion model	I	17.25	11.46	8.721	6.512
	R^2	0.781	0.744	0.756	0.751
	SSE	9.416	10.72	8.457	9.144
	SAE	8.238	9.148	11.72	10.459
	ARE	12.41	13.71	12.46	8.234
	HYBRID	11.56	9.854	11.73	9.243
	MPSD	9.843	11.23	9.546	10.325

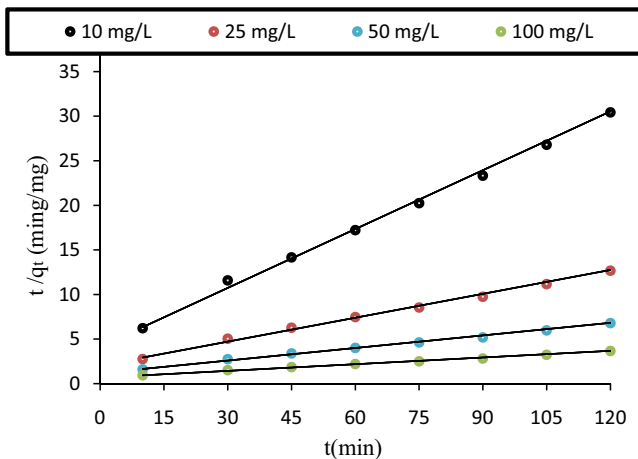


Fig. 8. Pseudo-second-order kinetic plots for adsorption of CIP on AFAC.

the plot at 303 K. The effect of the boundary layer increases as the value of I increases [19,20]. The boundary layer also gives information about the tendency of the adsorbent to either absorb the CIP particles or remain in the solution.

The higher the I values (boundary layer thickness), the higher the adsorption capacities (Table 2).

3.5. Adsorption isotherms

For the design of adsorption systems, the sorption isotherm models are very important because the isotherm models can provide maximum sorption capacity and expected interactions between adsorbate and adsorbents. In this study, four isotherm models (Langmuir, Freundlich, Dubinin–Radushkevich (D–R)) were applied to evaluate the equilibrium experimental data. Langmuir isotherm relates to monolayer adsorption of molecules. In the Langmuir isotherm model, maximum monolayer adsorption capacity, q_m (mg/g) and other parameters were determined from the following linearized form of Eq. (7) [33,44]:

$$\frac{C_e}{q_e} = \frac{1}{q_m b} + \frac{C_e}{q_m} \tag{7}$$

where C_e is the equilibrium concentration of the CIP in solution (mg/L), q_e is the adsorption capacity at equilibrium (mg/g), b (L/mg) Langmuir constants, related to the binding constant and q_m (mg/g) is the maximum adsorption

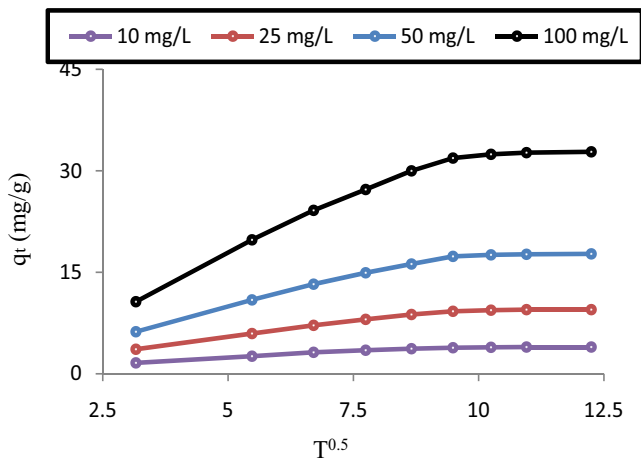


Fig. 9. Intraparticle diffusion kinetic plots for adsorption of CIP on AFAC.

capacity. A plot of specific sorption (C_e/q_e) vs. C_e (figure not shown) gives a straight line of slope ($1/q_m$) and intercepts ($1/q_m b$) as given in Table 2.

The Freundlich isotherm is expressed as Eq. (8) [45]:

$$\log q_e = \frac{1}{n} \log C_e + \log K_F \quad (8)$$

where K_F and n are Freundlich constants that are related to the bonding energy. K_F is the adsorption coefficient indicating the quantity of CIP adsorbed onto adsorbent for a unit equilibrium concentration. $1/n$ indicates the adsorption intensity of CIP onto the adsorbent with the adsorbent considered more heterogeneous as $1/n$ is closer to zero.

The relation between $\log q_e$ and $\log C_e$ (figure not shown) was significantly correlated. Table 2 represents the evaluated constants. The value $n = 1.745$ in the range of 1–10, indicates favorable adsorption.

The D–R model was also applied to estimate the characteristic porosity of the adsorbent, the apparent energy of adsorption and the characteristics of adsorption on micropores rather than on layer-by-layer adsorption. The D–R model is expressed as Eq. (9) [46]:

$$\ln q_e = \ln q_m - K\varepsilon^2 \quad (9)$$

where K indicates the adsorption energy constant, q_m represents the theoretical saturation capacity (mg/g), and ε is the Polanyi potential, calculated from Eq. (10) [46]:

$$\varepsilon = RT \ln \left(1 + \frac{1}{C_e} \right) \quad (10)$$

The constant K is expressed by the slope of the plot of $\ln q_e$ vs. ε^2 (figure not shown), and the adsorption capacity, q_m (mg/g) is represented by the intercept.

The mean free energy of adsorption, E (kJ/mol), was calculated using Eq. (11) [47]:

$$E = \frac{1}{\sqrt{2K}} \quad (11)$$

This can be used to estimate the type of adsorption. If the value is in the range of 8–16 kJ/mol, then the adsorption type can be explained by ion exchange, and if $E < 8$, the adsorption type is physisorption. The value of E calculated using above Eq. (11) was 2.25 kJ/mol for AFAC. This implies that the type of adsorption involved in this study is physisorption (physical sorption) which usually takes place at low temperatures.

3.6. Error analysis

The best isotherm model is determined by the correlation coefficient (R^2) analysis. Although this is useful in determining the efficiency of the correlation analysis, this analysis has limitations in solving isotherm models that are not inherently linear. Therefore, we used five error functions to find a suitable model to represent the experimental data [48,49]. The error functions we used is expressed as Eqs. (12)–(16).

$$SSE = \sum_{i=1}^n (q_{e,cal} - q_{e,meas})_i^2 \quad \text{Sum of Squared Errors} \quad (12)$$

$$SAE = \sum_{i=1}^n (q_{e,cal} - q_{e,meas})_i \quad \text{Sum of absolute errors} \quad (13)$$

$$ARE = \frac{100}{n} \sum_{i=1}^n \left(\frac{q_{e,cal} - q_{e,meas}}{q_{e,meas}} \right)_i \quad \text{Average relative error} \quad (14)$$

$$HYBRID = \frac{100}{n-p} \sum_{i=1}^n \left[\frac{(q_{e,meas} - q_{e,cal})_i^2}{q_{e,meas}} \right] \quad \text{Hybrid fractional error function} \quad (15)$$

$$MPSD = 100 \sqrt{\frac{1}{n-p} \sum_{i=1}^n \left(\frac{q_{e,meas} - q_{e,cal}}{q_{e,meas}} \right)_i^2} \quad \text{Marquart's percentage standard deviation} \quad (16)$$

Table 3 shows that the highest correlation coefficient was in the order of Langmuir, D–R, and Freundlich models. Based on these results, we concluded that the Langmuir isotherms displayed the lowest values of the error function. This suggests that the Langmuir isotherms fits the results better than the other models. Table 4 shows a comparison of the adsorption capacity (q_e) of different materials reported in the articles as adsorbent for CIP adsorption from aqueous solution under different experimental conditions.

3.7. Thermodynamic studies

The thermodynamics of the adsorption process was also investigated. The thermodynamic parameters such as entropy (ΔS°), enthalpy (ΔH°), standard Gibb's free energy (ΔG°) were obtained using the following equations.

$$K_0 = \frac{q_e}{C_e} \quad (17)$$

$$\Delta G^\circ = -RT \ln K_0 \quad (18)$$

Table 3
Isotherm models and error analysis parameters for CIP adsorption onto AFAC

Langmuir model		Freundlich model		D–R model	
q_m	35.14	n	1.745	q_m	38.83
b	0.395	K_f	5.056	K	0.0141
R^2	0.998	R^2	0.872	E	2.25
SSE	1.161	SSE	10.22	R^2	0.912
SAE	0.925	SAE	9.611	SSE	4.512
ARE %	3.115	ARE %	7.725	SAE	7.157
HYBRID	2.343	HYBRID	8.381	ARE	9.816
MPSD	1.632	MPSD	10.317	HYBRID	8.393

$$\ln K_0 = \left(\frac{\Delta S^\circ}{R} \right) - \left(\frac{\Delta H^\circ}{RT} \right) \quad (19)$$

where R is the gas constant (8.314 J/mol K), T is the absolute temperature (K). ΔH° and ΔS° were obtained as the gradient and intercept of the plot of $\ln K$ against $1/T$ respectively (Fig. 10).

The ΔS° , ΔG° and ΔH° are important parameters in assessing the thermodynamics of the adsorption systems, and these parameters are presented in Table 5. Negative Gibb's free energy value showed that the sorption process was both spontaneous and feasible. The values of ΔG° decreased from -0.079 to -5.61 kJ/mol as temperature increased. This suggests that the driving force increased at a higher temperature, which increases the level of adsorbate uptake. Positive entropy value, that is, ($\Delta S^\circ = 0.178$ kJ/mol) indicated increased randomness at the adsorbate–adsorbent interface. Also, the positive $\Delta H^\circ = 52.70$ kJ/mol confirmed the process to be endothermic.

3.8. Regeneration studies

To make the material more economical, the desorption of adsorbed CIP was of great significance for the reuse of adsorbents. The desorption efficiency of the AFAC was evaluated by performing adsorption–desorption experiments for five consecutive cycles. The results of the desorption

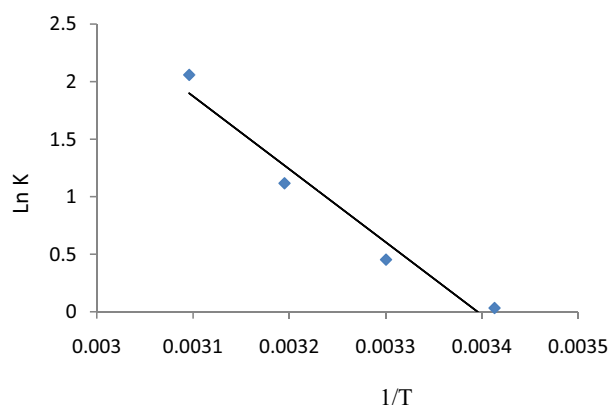


Fig. 10. Van't Hoff plot for the adsorption of CIP removal.

Table 5
Values of thermodynamic parameters for the adsorption of CIP onto AFAC

Temperature (K)	ΔG° (kJ/mol)	ΔH° (kJ/mol)	ΔS° (kJ/mol K)
293	-0.079		
303	-1.12		
313	-2.9	52.7	0.178
323	-5.61		

showed that higher desorption (91.5%) when H_2SO_4 is used, while the percentage of desorption was 84.5% and 28% when HCl and H_2O were used, respectively. The removal efficiency of AFAC in each adsorption cycle is shown in Fig. 11. The removal efficiency of all cycles remained almost unchanged, and from the first to the fifth stage, about a 7% reduction in removal rate was observed.

4. Conclusion

The removal efficiency of CIP by AFAC increased with increasing contact time, shaking speed, and CIP amount. The removal efficiency of CIP reached maxima (almost 100%) in 75 min. Similarly, the adsorption rate reached

Table 4
Comparison of the maximum adsorption of various adsorbent for CIP

Adsorbents	q_e (mg/g)	Reference	Adsorbents	q_e (mg/g)	Reference
AC-palm leaflets	48.91	[26]	Multi-walled carbon nanotubes (MWCNTs)	112.5	[4]
Granular AC	28.25	[7]	Synthesized NiO	81.29	[10]
Schorl	56.95	[8]	Magnetic-AC	29.19	[27]
MgO nanoparticles	84.93	[9]	CuO nanoparticles	89.46	[45]
SBA-15	45.19	[36]	Carbon xerogel	74.34	[3]
Kaolinitic clay	21.76	[49]	Coal fly ash	29.14	[30]
Birnessite	66.79	[26]	Bamboo charcoal	59.35	[50]
Hazelnut-AC	31.25	[5]	AFAC	35.14	This study

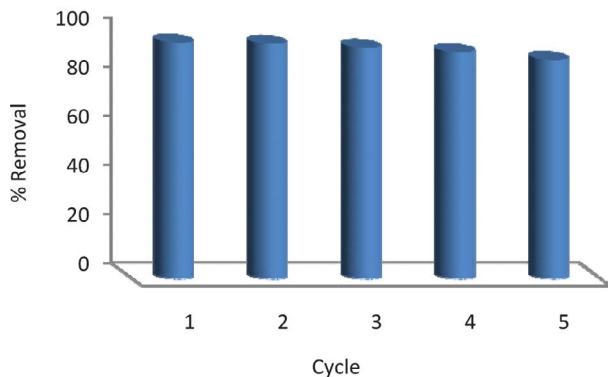


Fig. 11. Adsorption-desorption cycles of CIP onto AFAC.

maximum efficiency when the AFAC dose was 2.5 g/L. Based on the kinetic data, the pseudo-second-order model was able to describe the adsorption kinetics of the CIP. The linear regressions with five error functions revealed that the CIP adsorption onto AFAC best fitted the Langmuir isotherm in terms of the R^2 and error values. Thermodynamic studies showed that the adsorption process was spontaneous and endothermic, and followed a physisorption mechanism. Therefore, AFAC was found to be a suitable alternative to other adsorbents in removing CIP from aqueous solutions.

Acknowledgments

The authors are grateful to the Zahedan University of Medical Sciences for the financial support of this study (Code: 10288). This research was supported by the Basic Science Research Program through the National Research Foundation of Korea (NRF) funded by the Ministry of Education (NRF-2019R111A3A0106242412).

References

- [1] D. Balarak, F.K. Mostafapour, Photocatalytic degradation of amoxicillin using UV/Synthesized NiO from pharmaceutical wastewater, *Indonesian J. Chem.*, 19 (2019) 211–218.
- [2] N. Sharma, N. Dehiman, Kinetic and thermodynamic studies for ciprofloxacin hydrochloride adsorption from aqueous solution on CuO nanoparticles, *Int. J. ChemTech Res.*, 10 (2017) 98–106.
- [3] S.A.C. Carabineiro, T. Thavorn-Amornsri, M.F.R. Pereira, P. Serp, J.L. Figueiredo, Comparison between activated carbon, carbon xerogel and carbon nanotubes for the adsorption of the antibiotic ciprofloxacin, *Catal. Today*, 186 (2012) 29–34.
- [4] S.A.C. Carabineiro, T. Thavorn-Amornsri, M.F.R. Pereira, J.L. Figueiredo, Adsorption of ciprofloxacin on surface-modified carbon materials, *Water Res.*, 45 (2011) 4583–4591.
- [5] D. Balarak, H. Azarpira, F.K. Mostafapour, Adsorption kinetics and equilibrium of ciprofloxacin from aqueous solutions using *Corylus avellana* (Hazelnut) activated carbon, *Int. J. Pharm. Technol.*, 8 (2016) 16664–16675.
- [6] D. Avisar, O. Primor, I. Gozlan, H. Mamane, Sorption of sulfonamides and tetracyclines to montmorillonite clay, *Water Air Soil Pollut.*, 209 (2010) 439–450.
- [7] X. Zhu, D.C.W. Tsang, F. Chen, S. Li, X. Yang, Ciprofloxacin adsorption on graphene and granular activated carbon: kinetics, isotherms, and effects of solution chemistry, *Environ. Technol.*, 36 (2015) 3094–3102.
- [8] D. Yin, Z. Xu, J. Shi, L. Shen, Z. He, Adsorption characteristics of ciprofloxacin on the schorl: kinetics, thermodynamics, effect of metal ion and mechanisms, *J. Water Reuse Desal.*, 8 (2017) 350–359.
- [9] A. Fakhri, S. Adami, Adsorption and thermodynamic study of cephalosporins antibiotics from aqueous solution onto MgO nanoparticles, *J. Taiwan Inst. Chem. Eng.*, 45 (2014) 1001–1006.
- [10] D. Balarak, A.H. Mahvi, M.J. Shim, S.-M. Lee, Adsorption of ciprofloxacin from aqueous solution onto synthesized NiO: isotherm, kinetic and thermodynamic studies, *Desal. Water Treat.*, 203 (2020) 1–11.
- [11] H. Azarpira, Y. Mahdavi, O. Khaleghi, D. Balarak, Thermodynamic studies on the removal of metronidazole antibiotic by multi-walled carbon nanotubes, *Pharm. Lett.*, 8 (2016) 107–113.
- [12] J.M. Cha, S. Yang, K.H. Carlson, Trace determination of β -lactam antibiotics in surface water and urban wastewater using liquid chromatography combined with electrospray tandem mass spectrometry, *J. Chromatogr., A*, 1115 (2006) 46–57.
- [13] A.J. Watkinson, E.J. Murby, D.W. Kolpin, S.D. Costanzo, The occurrence of antibiotics in an urban watershed: from wastewater to drinking water, *Sci. Total Environ.*, 407 (2009) 2711–2723.
- [14] T.B. Minh, H.W. Leung, I.H. Loi, W.H. Chan, M.K. So, J.Q. Mao, D. Choi, J.C.W. Lam, G. Zheng, M. Martin, J.H.W. Lee, P.K.S. Lam, B.J. Richardson, Antibiotics in the Hong Kong metropolitan area: ubiquitous distribution and fate in Victoria Harbour, *Mar. Pollut. Bull.*, 58 (2009) 1052–1062.
- [15] X.L. Pan, C.N. Deng, D.Y. Zhang, J.L. Wang, G.J. Mu, Y. Chen, Toxic effects of amoxicillin on the photosystem II of *Synechocystis* sp. characterized by a variety of in vivo chlorophyll fluorescence tests, *Aquat. Toxicol.*, 89 (2008) 207–213.
- [16] H. Tekin, O. Bilkay, S.S. Ataberk, T.H. Balta, I.H. Ceribasi, F.D. Sanin, U. Yetis, Use of Fenton oxidation to improve the biodegradability of a pharmaceutical wastewater, *J. Hazard. Mater.*, 136 (2006) 258–265.
- [17] D. Balarak, H. Azarpira, Photocatalytic degradation of sulfamethoxazole in water: investigation of the effect of operational parameters, *Int. J. ChemTech Res.*, 9 (2016) 566–573.
- [18] X.S. Wang, Y. Zhou, Y. Jiang, C. Sun, The removal of basic dyes from aqueous solutions using agricultural by-products, *J. Hazard. Mater.*, 157 (2008) 374–385.
- [19] L.A. Al-Khateeb, S. Almotiry, M.A. Salam, Adsorption of pharmaceutical pollutants onto graphene nanoplatelets, *Chem. Eng. J.*, 248 (2014) 191–199.
- [20] W.-T. Jiang, P.-H. Chang, Y.-S. Wang, Y.L. Tsai, J.-S. Jean, Z.H. Li, K. Krukowski, Removal of ciprofloxacin from water by birnessite, *J. Hazard. Mater.*, 250 (2013) 362–369.
- [21] K. Shalini, S.Z. Anwer, P.K. Sharma, V.K. Garg, N. Kumar, A review on pharmaceutical pollution, *Int. J. PharmTech. Res.*, 2 (2010) 2265.
- [22] J.L. Santos, I. Aparicio, E. Alonso, Occurrence and risk assessment of pharmaceutically active compounds in wastewater treatment plants. A case study: Seville City (Spain), *Environ. Int.*, 33 (2007) 596–601.
- [23] K. Oberle, M.J. Capdeville, T. Berthe, H. Budzinski, F. Petit, Evidence for a complex relationship between antibiotics and antibiotic-resistant *Escherichia coli*: from medical center patients to a receiving environment, *Environ. Sci. Technol.*, 46 (2012) 1859–1868.
- [24] R. Noroozi, T.J. Al-Musawi, H. Kazemian, E.M. Kalhori, M. Zarrabi, Removal of cyanide using surface-modified Linde Type-A zeolite nanoparticles as an efficient and eco-friendly material, *J. Water Process Eng.*, 21 (2018) 44–51.
- [25] J. Deng, Y. Shao, N. Gao, C. Tan, S. Zhou, X. Hu, CoFe_2O_4 magnetic nanoparticles as a highly active heterogeneous catalyst of oxone for the degradation of diclofenac in water, *J. Hazard. Mater.*, 262 (2013) 836–844.
- [26] E.-S.I. El-Shafey, H. Al-Lawati, A.S. Al-Sumri, Ciprofloxacin adsorption from aqueous solution onto chemically prepared carbon from date palm leaflets, *J. Environ. Sci.*, 24 (2012) 1579–1586.

- [27] S.T. Danaloğlu, S.S. Bayazit, O.K. Kuyumcu, M.A. Salam, Efficient removal of antibiotics by a novel magnetic adsorbent: magnetic activated carbon/chitosan (MACC) nanocomposite, *J. Mol. Liq.*, 240 (2017) 589–596.
- [28] R.A. Diyanati, Z. Yousefi, J.Y. Cherati, The ability of *Azolla* and *Lemna minor* biomass for adsorption of phenol from aqueous solutions, *J. Mazand Univ. Med. Sci.*, 23 (2013) 17–23.
- [29] M.A. Zazouli, A.H. Mahvi, S. Dobaradaran, M. Barafrahshtehpour, Y. Mahdavi, Adsorption of fluoride from aqueous solution by modified *Azolla filiculoides*, *Fluoride*, 47 (2014) 349–358.
- [30] R.A. Diyanati, Z. Yousefi, J.Y. Cherati, Investigating phenol adsorption from aqueous solution by dried *Azolla*, *J. Mazand Univ. Med. Sci.*, 22 (2013) 13–21.
- [31] C.L. Zhang, G.L. Qiao, F. Zhao, Y. Wang, Thermodynamic and kinetic parameters of ciprofloxacin adsorption onto modified coal fly ash from aqueous solution, *J. Mol. Liq.* 163 (2011) 53–56.
- [32] S. Rakshit, D. Sarkar, E.J. Elzinga, P. Punamiya, R. Datta, Mechanisms of ciprofloxacin removal by nano-sized magnetite, *J. Hazard. Mater.*, 246 (2013) 221–226.
- [33] D. Balarak, E. Bazrafshan, Y. Mahdavi, S.M. Lee, Kinetic, isotherms and thermodynamic studies in the removal of 2-chlorophenol from aqueous solution using modified rice straw, *Desal. Water Treat.*, 63 (2017) 203–211.
- [34] D. Balarak, F. Mostafapour, E. Bazrafshan, T.A. Saleh, Studies on the adsorption of amoxicillin on multi-wall carbon nanotubes, *Water Sci. Technol.*, 75 (2017) 1599–1606.
- [35] A.A. Mohammadi, A. Zarei, H. Alidadi, M. Afsharnia, M. Shams, Two dimensional zeolitic imidazolate framework-8 for efficient removal of phosphate from water, process modeling, optimization, kinetic, and isotherm studies, *Desal. Water Treat.*, 129 (2018) 244
- [36] W.R.D.N. Sousa, A.R. Oliveira, J.F.C. Filho, T.C.M. Dantas, A.G.D. Santos, V.P.S. Caldeira, E.L. Geraldo, Ciprofloxacin adsorption on ZnO supported on SBA-15, *Water Air Soil Pollut.*, 229 (2018) 1–12.
- [37] Y.J. Tu, C.F. You, M.H. Chen, Y.P. Duan, Efficient removal/recovery of Pb onto environmentally friendly fabricated copper ferrite nanoparticles, *J. Taiwan Inst. Chem. Eng.*, 71 (2017) 197–205.
- [38] Y. Tang, H. Guo, L. Xiao, S. Yu, N. Gao, Y. Wang, Synthesis of reduced graphene oxide/magnetite composites and investigation of their adsorption performance of fluoroquinolone antibiotics, *Colloids Surf., A*, 424 (2013) 74–80.
- [39] H. Chen, Z. Zhang, M. Feng, W. Liu, W. Wang, Q. Yang, Y. Hu, Degradation of 2,4-dichlorophenoxyacetic acid in water by persulfate activated with FeS (Mackinawite), *Chem. Eng. J.*, 313 (2017) 498–507.
- [40] B.N. Estevinho, I. Martins, N. Ratola, A. Alves, L. Santos, Removal of 2,4-dichlorophenol and pentachlorophenol from waters by sorption using coal fly ash from a Portuguese thermal power plant, *J. Hazard. Mater.*, 143 (2007) 535–540.
- [41] A.H. Mahvi, F.K. Mostafapour, Biosorption of tetracycline from aqueous solution by *Azolla filiculoides*: equilibrium kinetic and thermodynamic studies, *Fresenius Environ. Bull.*, 27 (2018) 5759–5767.
- [42] D. Balarak, H. Azarpira, F.K. Mostafapour, Adsorption isotherm studies of tetracycline antibiotics from aqueous solutions by maize stalks as a cheap biosorbent, *Int. J. Pharm. Technol.*, 8 (2016) 16664–16675.
- [43] Y. Gao, Y. Li, L. Zhang, H. Huang, J. Hu, S.M. Shah, X. Su, Adsorption and removal of tetracycline antibiotics from aqueous solution by graphene oxide, *J. Colloid Interface Sci.*, 368 (2012) 540–546.
- [44] M.E. Parolo, M.C. Savini, J.M. Vallés, M.T. Baschini, M.J. Avena, Tetracycline adsorption on montmorillonite: pH and ionic strength effects, *Appl. Clay Sci.*, 40 (2008) 179–186.
- [45] S. Ahmadi, A. Banach, F.K. Mostafapour, Study survey of cupric oxide nanoparticles in removal efficiency of ciprofloxacin antibiotic from aqueous solution: adsorption isotherm study, *Desal. Water Treat.*, 89 (2017) 297–303.
- [46] D. Balarak, H. Azarpira, Rice husk as a biosorbent for antibiotic metronidazole removal: isotherm studies and model validation, *Int. J. ChemTech Res.*, 9 (2016) 566–573.
- [47] L.T. Popoola, Tetracycline and sulfamethoxazole adsorption onto nanomagnetic walnut shell-rice husk: isotherm, kinetic, mechanistic and thermodynamic studies, *Int. J. Environ. Anal. Chem.*, 100 (2019) 1–23.
- [48] D. Balarak, H. Azarpira, F.K. Mostafapour, Study of the adsorption mechanisms of cephalexin on to *Azolla filiculoides*, *Pharm. Chem.*, 8 (2016) 114–121.
- [49] F.A. Adekola, H.I. Adegoke, G.B. Adebayo, I.O. Abdulsalam, Batch sorption of ciprofloxacin on kaolinitic clay and rhematite composite: equilibrium and thermodynamics studies, *Mor. J. Chem.*, 4 (2016) 384–424.
- [50] L. Wang, G. Chen, C. Ling, J. Zhang, K. Szerlag, Adsorption of ciprofloxacin on to bamboo charcoal: effects of pH, salinity, cations, and phosphate, *Environ. Prog. Sustainable Energy*, 36 (2017) 1108–1115.